

# Geophysical Research Letters<sup>®</sup>






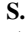


## RESEARCH LETTER

10.1029/2023GL106958

## Byrd Ice Core Debris Constrains the Sediment Provenance Signature of Central West Antarctica

### Key Points:

- Debris from the base of the Byrd ice core comprises predominantly of sedimentary strata weathered before the onset of Antarctic glaciation
- <sup>40</sup>Ar/<sup>39</sup>Ar dated hornblende grains support evidence for recent subglacial volcanism
- Byrd geochemical data reveal the provenance signature expected in marine sediments following major West Antarctic Ice Sheet retreat

J. W. Marschalek<sup>1</sup> , P.-H. Blard<sup>2,3</sup> , E. Sarigulyan<sup>2</sup> , W. Ehrmann<sup>4</sup> , S. R. Hemming<sup>5</sup> , S. N. Thomson<sup>6</sup> , C.-D. Hillenbrand<sup>7</sup> , K. Licht<sup>8</sup> , J.-L. Tison<sup>3</sup> , L. Ardoin<sup>3</sup> , F. Fripiat<sup>3</sup>, C. S. Allen<sup>7</sup> , Y. Marrocchi<sup>2</sup>, M. J. Siegert<sup>1,9</sup> , and T. van de Flierdt<sup>1</sup> 

<sup>1</sup>Department of Earth Science and Engineering, Imperial College London, London, UK, <sup>2</sup>CRPG, CNRS, Université de Lorraine, Nancy, France, <sup>3</sup>Laboratoire de Glaciologie, Université Libre de Bruxelles, Brussels, Belgium, <sup>4</sup>Institute of Geophysics and Geology, University of Leipzig, Leipzig, Germany, <sup>5</sup>Lamont-Doherty Earth Observatory of Columbia University Palisades, New York, NY, USA, <sup>6</sup>Department of Geosciences, University of Arizona, Tucson, AZ, USA, <sup>7</sup>British Antarctic Survey, Cambridge, UK, <sup>8</sup>Department of Earth and Environmental Sciences, Indiana University Indianapolis, Indianapolis, IN, USA, <sup>9</sup>Tremough House, University of Exeter, Cornwall, UK

### Supporting Information:

Supporting Information may be found in the online version of this article.

### Correspondence to:

J. W. Marschalek,  
jwm17@ic.ac.uk

### Citation:

Marschalek, J. W., Blard, P.-H., Sarigulyan, E., Ehrmann, W., Hemming, S. R., Thomson, S. N., et al. (2024). Byrd ice core debris constrains the sediment provenance signature of central West Antarctica. *Geophysical Research Letters*, 51, e2023GL106958. <https://doi.org/10.1029/2023GL106958>

Received 26 OCT 2023

Accepted 21 FEB 2024

### Author Contributions:

**Conceptualization:** J. W. Marschalek, P.-H. Blard, C.-D. Hillenbrand, K. Licht, J.-L. Tison, M. J. Siegert, T. van de Flierdt  
**Data curation:** J. W. Marschalek, S. N. Thomson

**Formal analysis:** J. W. Marschalek, P.-H. Blard, E. Sarigulyan, W. Ehrmann, S. R. Hemming, S. N. Thomson, J.-L. Tison, L. Ardoin, F. Fripiat, C. S. Allen, Y. Marrocchi

**Funding acquisition:** P.-H. Blard, J.-L. Tison, M. J. Siegert, T. van de Flierdt

**Investigation:** C.-D. Hillenbrand

**Resources:** P.-H. Blard, W. Ehrmann, S. R. Hemming, S. N. Thomson, C.-D. Hillenbrand, K. Licht, C. S. Allen, T. van de Flierdt

© 2024. The Authors.

This is an open access article under the terms of the [Creative Commons Attribution License](https://creativecommons.org/licenses/by/4.0/), which permits use, distribution and reproduction in any medium, provided the original work is properly cited.

**Abstract** Provenance records from sediments deposited offshore of the West Antarctic Ice Sheet (WAIS) can help identify past major ice retreat, thus constraining ice-sheet models projecting future sea-level rise. Interpretations from such records are, however, hampered by the ice obscuring Antarctica's geology. Here, we explore central West Antarctica's subglacial geology using basal debris from within the Byrd ice core, drilled to the bed in 1968. Sand grain microtextures and a high kaolinite content (~38–42%) reveal the debris consists predominantly of eroded sedimentary detritus, likely deposited initially in a warm, pre-Oligocene, subaerial environment. Detrital hornblende <sup>40</sup>Ar/<sup>39</sup>Ar ages suggest proximal late Cenozoic subglacial volcanism. The debris has a distinct provenance signature, with: common Permian–Early Jurassic mineral grains; absent early Ross Orogeny grains; a high kaolinite content; and high <sup>143</sup>Nd/<sup>144</sup>Nd and low <sup>87</sup>Sr/<sup>86</sup>Sr ratios. Detecting this “fingerprint” in Antarctic sedimentary records could imply major WAIS retreat, revealing the WAIS's sensitivity to future warming.

**Plain Language Summary** Ice loss from the West Antarctic Ice Sheet (WAIS) could potentially raise global sea level by up to 4 m over the coming decades to centuries. However, projections of sea-level contributions from the WAIS are highly uncertain. Understanding when the WAIS was smaller in warm times in the Earth's more recent history would reduce these uncertainties, but direct evidence for the most recent large-scale WAIS retreat is lacking. Tracing the source of sediments deposited offshore will help detect WAIS retreat because, under a smaller WAIS, there would be more erosion of presently ice-covered areas in central West Antarctica. However, the subglacial geology of central West Antarctica is poorly known, making it difficult to identify a WAIS retreat signal in sedimentary records. Here, we present new results from debris in the Byrd ice core, drilled in the center of the WAIS to its base in 1968. The mineralogical, geochemical and age compositions of the debris provide a distinct geological “fingerprint” that should be identifiable in sedimentary records. This fingerprint can be searched for in existing and upcoming Antarctic drill core records, which will ultimately help constrain the environmental conditions that would lead to future WAIS retreat and the resulting sea-level rise.

## 1. Introduction

Understanding when full or partial collapses of the West Antarctic Ice Sheet (WAIS) occurred in the past is key for constraining the environmental thresholds leading to future ice loss and sea-level rise. Despite the importance of reconstructing past changes in WAIS extent and volume, no conclusive ice-proximal evidence has yet been found for major WAIS retreat (i.e., retreat of the ice sheet margin hundreds of kilometers inland of its modern position) during times of recent warmth, such as the Last Interglacial (Dutton et al., 2015; Dutton & Lambeck, 2012).

Sediment provenance characteristics in Antarctic sediment cores constitute an important method for detecting major ice sheet retreat (e.g., Cook et al., 2013). This approach makes use of the fact that ice sheet retreat would change the spatial pattern of subglacial erosion by promoting faster basal velocities further inland toward the modern ice divide. This would lead to the erosion and transportation of different rock sources. However, the

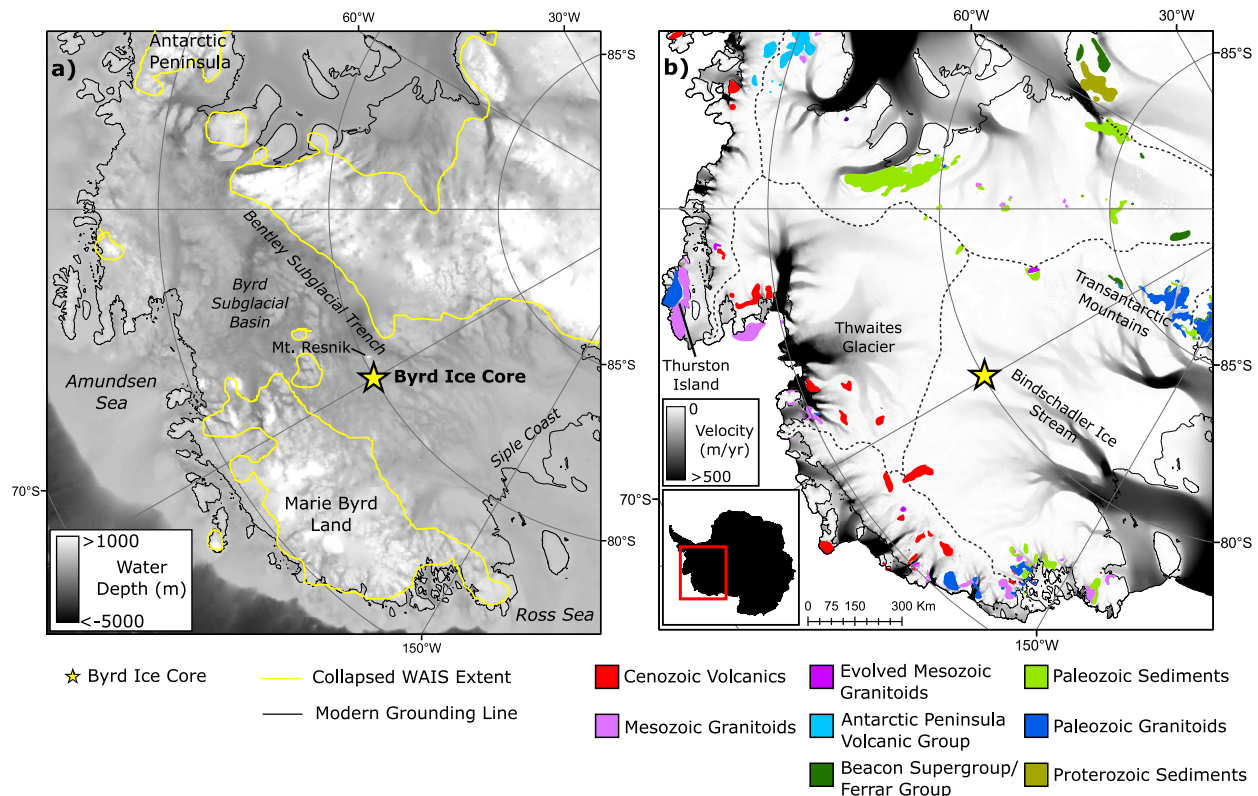
**Supervision:** C.-D. Hillenbrand, M. J. Siegert, T. van de Flierdt  
**Validation:** T. van de Flierdt  
**Visualization:** J. W. Marschalek, P.-H. Blard, E. Sarigulyan  
**Writing – original draft:** J. W. Marschalek, P.-H. Blard, E. Sarigulyan, C.-D. Hillenbrand, M. J. Siegert, T. van de Flierdt  
**Writing – review & editing:** J. W. Marschalek, P.-H. Blard, W. Ehrmann, S. R. Hemming, C.-D. Hillenbrand, K. Licht, J.-L. Tison, L. Ardoin, F. Fripiat, C. S. Allen, Y. Marrocchi, M. J. Siegert, T. van de Flierdt

ability for sediment provenance studies to detect major WAIS retreat is severely hampered by a lack of knowledge of the geology below the ice-covered WAIS interior (Figure 1b).

Improved characterization of the geology of the West Antarctic interior can be gained using geophysical techniques (e.g., Behrendt, 1999, 2013; Jordan et al., 2023) and studies of marine sediments (e.g., Andrews & LeMasurier, 2021; Simões Pereira et al., 2018). However, inspection of debris recovered by drilling to the ice sheet's base refines the spatial extent of rock types and is therefore indispensable to unraveling local geology (e.g., Farmer et al., 2006; Licht et al., 2014).

The Byrd ice core (80° 0.1'S, 119° 31.0'W) penetrated 2,146 m of ice at Byrd Station in January 1968 (Gow et al., 1968) at the junction between the Amundsen Sea and Ross Sea sectors of the WAIS, hundreds of kilometers from the nearest outcropping rock (Figure 1). A small quantity of englacial debris was recovered entrained within the lowermost 4.83 m of the ice; that is, the silty ice (Gow et al., 1979). Although liquid water was present at the ice column base when drilling, the stratification and low gas content of the silty ice suggest incorporation of the debris by “freeze-on” of glacially derived meltwater, permitted by temperatures at the ice-bed interface falling below the pressure-melting point (Christoffersen et al., 2006; Gow & Meese, 1996). The silty ice was accreted after ~100 ka, as it must post-date the meteoric ice above (Blunier & Brook, 2001; Johnsen et al., 1972).

Insight into the rock types present in the Byrd ice core debris has previously been gained by petrographic classification of pebble-sized clasts, limited x-ray diffraction analyses of the sand-clay fraction, sand fraction petrography, and two <sup>40</sup>Ar/<sup>39</sup>Ar dated pebbles (Gow et al., 1979; Vogel, 2004; Vogel et al., 2006). These studies suggest diverse lithologies are present within the debris, including granite, quartz-monzonite, basalt, tuff and arkosic arenite clasts (Gow et al., 1979). However, these studies did not identify the relative abundance of potential rock groups. Conceptually, these could include Cretaceous granitoids that outcrop elsewhere in West



**Figure 1.** Location of the Byrd ice core (yellow star) with subglacial topographic and geologic context in West Antarctica. (a) Subglacial topography (BedMachine V1 Antarctica; Morlighem et al., 2020), with the modern grounding line (black line) and a modeled Last Interglacial (125 ka) “collapsed” ice sheet extent (yellow line; Figure 3b of DeConto & Pollard, 2016). (b) Geological map of West Antarctica based on GeoMAP Antarctica (Cox et al., 2023) plotted on surface velocity data (Mouginot et al., 2019). Dashed lines indicate the main ice divides (Mouginot et al., 2017; Rignot et al., 2013). The inset shows the location of the main panels within Antarctica.

Antarctica (e.g., Weaver et al., 1992; Korhonen et al., 2010; Figure 1), igneous Permian-Triassic rocks inferred from detrital minerals to exist beneath the WAIS (Licht et al., 2014; Perotti et al., 2017; Simões Pereira et al., 2018, 2020) and Paleozoic (meta-)sedimentary strata found around West Antarctica (e.g., Storey & MacDonald, 1987; Korhonen et al., 2010; Figure 1).

Here, new techniques have been applied to provide novel insight into the rock types comprising the Byrd ice core debris. Methods are described in Supporting Information S1 and include petrographic observations, mineral characterization, and geochemical analyses.

## 2. Results

Three intervals were sampled from the Byrd ice core in August 2021 (Figure S1 in Supporting Information S1). Ascending from the ice-bed interface, sample heights above the ice-core base were approximately 86–101 cm (from Section 1408-B1), ~183–197 cm (from Section 1407-C2) and ~403–419.5 cm (from Section 1406-C2). These samples are henceforth referred to as “Lower,” “Middle,” and “Upper,” respectively. The debris comprises mainly of very fine to coarse sand (75–800  $\mu\text{m}$ ); clay, silt and extremely fine sand (<75  $\mu\text{m}$ ) were rare except for the Middle sample and their proportions were highly variable, comprising 1%, 28% and 4% of the mass of the debris, respectively (Table S1 in Supporting Information S1). This grain-size distribution matches earlier analyses of the Byrd debris (Vogel, 2004). A ~25 g rhyolite porphyry cobble was also retrieved from the Upper sample (~406 cm above the base).

### 2.1. Scanning Electron Microprobe (SEM) Imaging and X-Ray Mapping

SEM imaging revealed that all three debris samples contained predominantly sub-rounded to angular grains, consistent with sediment sourced from and mobilized within a glacial environment. Glacial microtextural features are abundant, including conchoidal fractures, linear steps, mechanically-upturned plates and glacial striations, consistent with transport in the present setting beneath ice >1,000 m thick (Mahaney, 1995, 2002; Figure 2).

Sand grains in all three samples also often have smoothed edges and surfaces showing signs of weathering (Figure 2). These weathered surfaces are cut by glacial microtextures (e.g., Figure 2a), implying the weathering predates the most recent abrasion by glacial ice (Figure 2). Also often present are clay mineral coatings, which indicate that percolating liquid water has been present (Mahaney, 2002). Salt crystals are also visible (Figure 2c), suggesting the presence of saline porewater. Coatings are less common and grains more angular in the Middle sample.

Whilst the Upper and Middle samples contain mainly monocrystalline grains showing strong evidence of glacial abrasion (Figures 2a–2f), the Lower sample contains few monocrystalline grains and is instead dominated by fine-grained aggregated particles (e.g., Figure 2i), which do not resemble described glacial aggregates (e.g., Cowan et al., 2012). The lack of monocrystalline grains means there are fewer hard crystal surfaces to show microtextures.

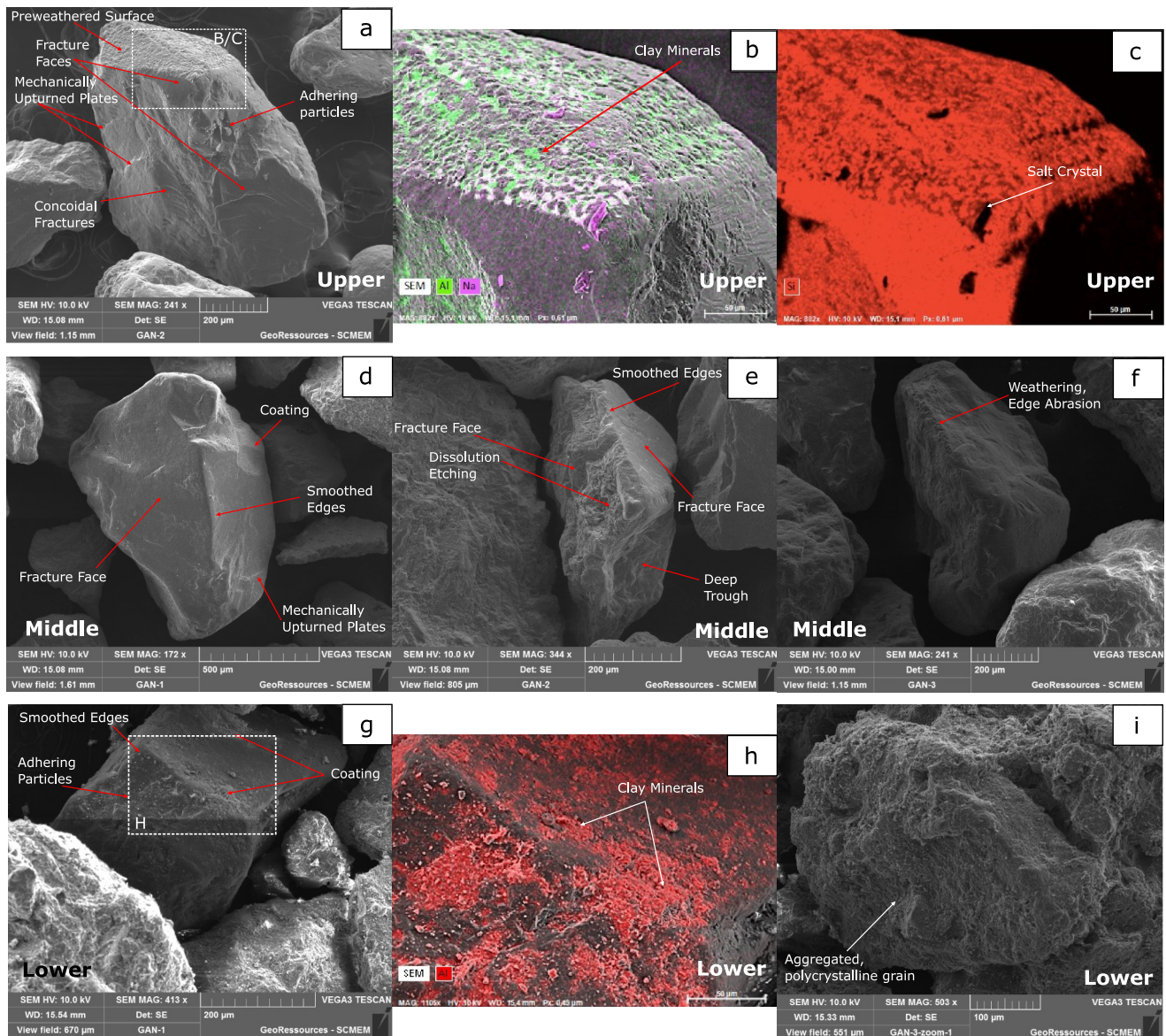
Electron microprobe analysis suggests all the samples were dominated by quartz and feldspar, with the Upper sample containing slightly more quartz and the Middle and Lower samples containing mostly feldspar (Table S2 in Supporting Information S1). The Upper sample also contains pyroxene, whereas in the Lower and Middle samples pyroxene is absent (Table S2 in Supporting Information S1).

### 2.2. Clay Mineralogy

Clay mineral compositions in the <2  $\mu\text{m}$  fraction are broadly similar at all three depths in the ice core, with samples containing 20%–25% smectite, 19%–24% illite, 16%–19% chlorite, and 37%–42% kaolinite (Figure 3c). Illite and chlorite are associated with physical weathering of a wide range of lithologies and would therefore be expected to be the dominant clay minerals in a subglacial setting. However, in the Byrd ice core debris, neither comprises >24% of the clay mineral assemblages, far less than the ~40% kaolinite contribution (Figure 3).

### 2.3. Neodymium and Strontium Isotopes

The range of the measured  $^{87}\text{Sr}/^{86}\text{Sr}$  ratios far exceeds the analytical error, varying from 0.7087 to 0.7145 and decreasing higher in the ice column (Figure 3b).  $^{143}\text{Nd}/^{144}\text{Nd}$  ratios are expressed as  $\epsilon_{\text{Nd}}$  values,

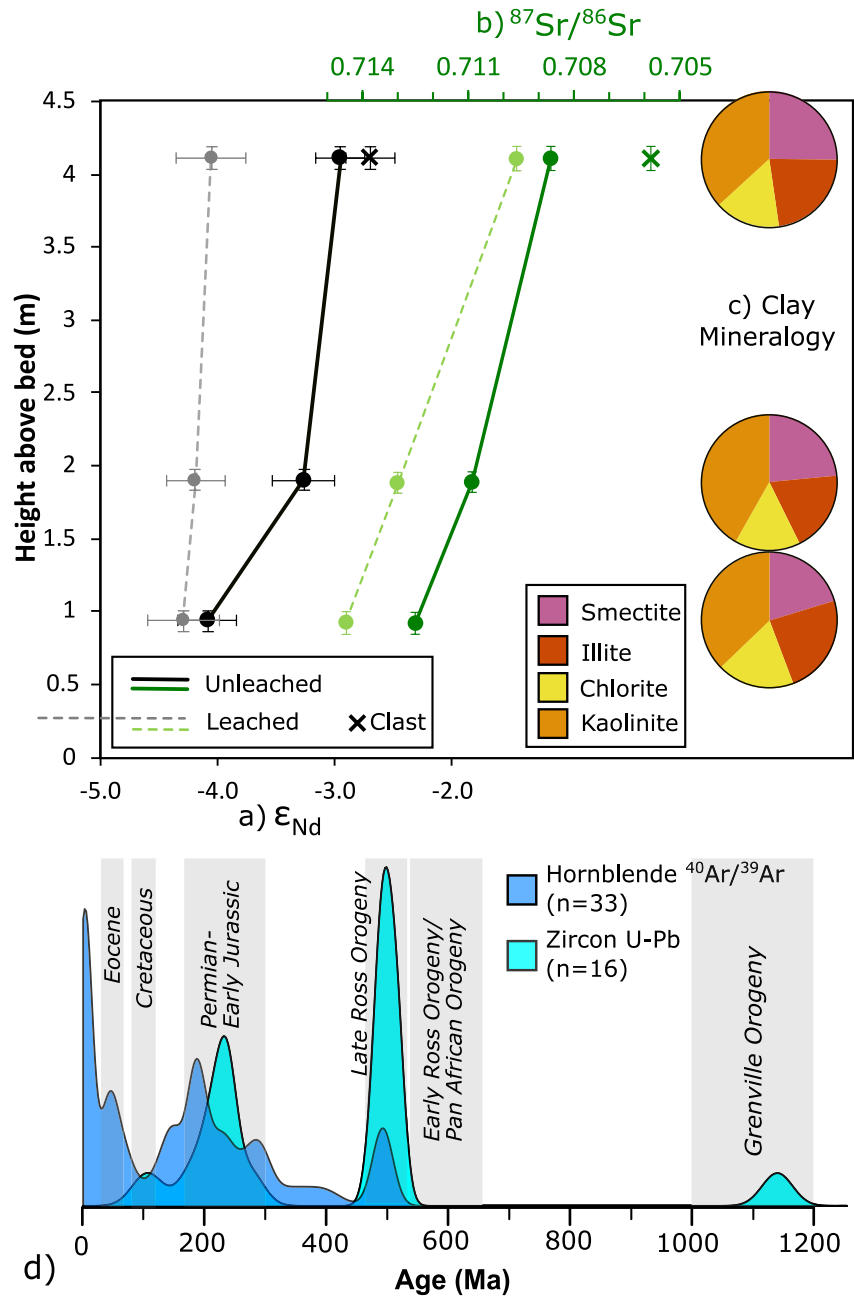


**Figure 2.** Selected SEM images and x-ray maps of 200–810  $\mu\text{m}$  grains. Grains are from the Upper (a–c), Middle (d–f) and Lower (g–i) samples. Key microtextural features are labeled and described in the text.

denoting the deviation from the modern Chondritic Uniform Reservoir (Jacobsen & Wasserburg, 1980). In the  $<75 \mu\text{m}$  fractions,  $\epsilon_{\text{Nd}}$  values increase with height in the ice column by  $\sim 1.3$  epsilon units ( $\epsilon_{\text{Nd}} = -3.0$  to  $-4.3$ ), a range well outside the maximum analytical error of 0.3 (Figure 3a). This trend with height is, however, largely removed by treatment with the leaching solution designed to remove authigenic mineral coatings (Section S2.1 in Supporting Information S1). These coatings must have  $\epsilon_{\text{Nd}}$  values higher (more radiogenic) and  $^{87}\text{Sr}/^{86}\text{Sr}$  ratios lower (less radiogenic) than the bulk composition; we speculate that they may have derived from dissolution and reprecipitation of more soluble mineral phases. The rhyolite clast has an  $\epsilon_{\text{Nd}}$  value of  $-2.7 \pm 0.2$  and an  $^{87}\text{Sr}/^{86}\text{Sr}$  ratio of  $\sim 0.7058$  (Figure 3).

#### 2.4. Zircon U-Pb, Hornblende $^{40}\text{Ar}/^{39}\text{Ar}$ and Apatite Fission Track Dating

Zircon, apatite and hornblende grains were picked from the 75–210  $\mu\text{m}$  size fractions (see details on grain size selection in Supporting Information S1). However, only the Upper and Middle samples contained datable grains, with the absence of suitable grains from the Lower sample likely due to the dominance of aggregated grains (e.g.,



**Figure 3.** Provenience characteristics of the Byrd ice core debris and changes with depth in the ice column. (a)  $\epsilon_{Nd}$  values of both leached (gray) and unleached (black) aliquots; (b)  $^{87}Sr/^{86}Sr$  ratios of both leached (green) and unleached (light green) aliquots (x-axis is reversed; horizontal error bars are smaller than the symbols); and (c) clay mineral composition. Crosses mark data from the rhyolite porphyry clast. (d) Kernel density estimates (Vermeesch, 2012) of the hornblende  $^{40}Ar/^{39}Ar$  (dark blue) and zircon U-Pb (light blue) ages, with both Upper and Middle sample data combined. As negative hornblende  $^{40}Ar/^{39}Ar$  ages are not physically plausible but reflect a geologically young contribution to the debris, they are assumed to be zero for plotting. Gray boxes indicate regionally significant age populations.

Figure 2i). Thirteen of the 16 zircon grains analyzed were found in the Upper sample. Hornblende grains were more plentiful and evenly distributed, with 56 and 73 grains picked from the Upper and Middle samples, respectively.

Zircon U-Pb dating results show a broad range of ages, with single grains from the Mesoproterozoic ( $1,138.0 \pm 5.0$  Ma) and the Cretaceous ( $105.5 \pm 0.9$  Ma) (Figure 3d). Eight of the 16 grains date to the youngest phase of the Ross Orogeny ( $\sim 520$ – $475$  Ma) and six grains date from the Permian–Early Jurassic ( $\sim 272$ – $180$  Ma).

Of the 129 hornblende grains irradiated for  $^{40}\text{Ar}/^{39}\text{Ar}$  dating, only 33 yielded sufficient  $^{39}\text{Ar}$  for reliable analytical results. This is likely linked to the small grain size used. Age populations span the Ross Orogeny ( $\sim 490$  Ma,  $n = 3$ ), Permian to Early Jurassic ( $292$ – $180$  Ma,  $n = 11$ ), Late Jurassic to Early Cretaceous ( $\sim 153$ – $135$  Ma,  $n = 3$ ) and Eocene ( $\sim 43$ – $41$  Ma,  $n = 3$ ). A further three grains gave Miocene ages ( $14$ – $6$  Ma) and five grains yielded nominally negative ages with errors overlapping zero (Table S3 in Supporting Information S1). These negative ages are likely to be geologically very young (i.e.,  $< \sim 1$  Ma) as their measured  $^{40}\text{Ar}/^{36}\text{Ar}$  ratios are very close to that of air. In addition, one grain yielded a Carboniferous age ( $338.4 \pm 7.4$  Ma) and one a mid-Cretaceous age ( $113.0 \pm 8.4$  Ma). The groundmass of the rhyolite porphyry clast yielded an integrated  $^{40}\text{Ar}/^{39}\text{Ar}$  age of  $\sim 218$  Ma but no formal plateau was achieved, implying some complexity in this age (Figure S2 in Supporting Information S1).

Apatite fission tracks were measured on 10 grains and yielded seven ages spanning  $\sim 112$ – $92$  Ma, with other grains dating to  $\sim 75$ ,  $72$ , and  $46$  Ma (Table S4 in Supporting Information S1). These mid- to late-Cretaceous and Eocene age populations are observed in many Ross Sea sediments, particularly toward the eastern Ross Sea (Li et al., 2020; Olivetti et al., 2023; Perotti et al., 2017).

### 3. Discussion

#### 3.1. Local Sedimentary Contribution From a Warm, Subaerial Setting

All evidence points to the Byrd ice core debris being predominantly eroded sedimentary material rather than primary erosion of crystalline bedrock. This includes: (a) dominance of kaolinite ( $\sim 40\%$ ) in the clay mineral assemblage (Figure 3c), which does not form (at least in such high abundance) in subglacial settings (see discussion below); (b) a mixture of clast lithologies (Gow et al., 1979); (c) a mixture of mineral grain ages spanning  $> 1,100$  Ma (Figure 3d); (d) the presence of fine/even-grained aggregated particles which do not appear glacial in origin (Figure 2i; Cowan et al., 2012); and (e) preweathered grain surfaces cut by more recent glacial textures (Figure 2). The age and depositional setting of this sedimentary component is explored below.

If the sedimentary material within the englacial debris was deposited during the mid to late Quaternary, it would indicate ungrounding of the ice sheet in the West Antarctic interior during this time interval (i.e., major WAIS retreat). Under such a scenario, marine diatom species with age ranges unique to the mid-late Quaternary could be present (cf. Scherer et al., 1998). Such species were carefully searched for in all samples, but no definitive diatoms of this age were found.

We hypothesize this absence of diatoms, which are sometimes found in Antarctic subglacial tills (e.g., Coenen et al., 2020), is due to the sedimentary component of the debris being deposited in a pre-Oligocene subaerial setting. This hypothesis is supported by the high abundance of kaolinite in the clay mineral assemblage ( $\sim 40\%$ ; Figure 3c). Although it has been suggested that a small amount of kaolinite may form subglacially (Graly et al., 2020), it is very unlikely to be the dominant clay mineral forming under the modern ice sheet as kaolinite formation requires low pH soil conditions typically associated with swamps and (sub)tropical climates (Huang & Keller, 1970; Klages et al., 2020; Petschick et al., 1996; Windom, 1976). When found offshore of Antarctica, kaolinite is assumed to be sourced from erosion of sedimentary strata pre-dating the onset of Antarctic glaciation in the earliest Oligocene (Ehrmann et al., 1992, 2011; Hambrey et al., 1991; Hillenbrand et al., 2003; Simões Pereira et al., 2020). As kaolinite is abundant in the Byrd ice core debris, a large proportion of the clay-sized fraction must derive from sediment deposited in a much warmer environment. Given the long-term positioning of the Antarctic continent at high latitudes, the kaolinite detected in the Byrd ice core debris supports evidence for swampy temperate conditions (Klages et al., 2020) and/or (sub)tropical conditions at very high latitudes in the past (Robert & Kennett, 1994).

The depositional environment of the sediment can be constrained using the SEM imagery. Specifically, clay mineral coatings present on sand grains often occur in depressions on preweathered surfaces but not on more recent glacially-cut surfaces (e.g., Figure 2b). This observation suggests these clays were likely generated in a palaeosol/subaerial setting (Blard et al., 2023; Mahaney, 2002). Particularly in the Lower sample, clay minerals may also derive from the aggregated grains present (Figure 2i). Clay mineral coatings are, however, occasionally

adhered to sand grain surfaces that are not highly weathered (e.g., Figure 2h), suggesting either subglacial till transport or limited clay mineral formation in a subglacial environment close to the pressure-melting point (e.g., Arnardottir et al., 2023).

These pre-Oligocene sedimentary strata are likely to be local to the Byrd ice core site. As the site is close to the modern-day Amundsen Sea/Ross Sea ice divide (Figure 1b), modeled basal ice velocities are very slow ( $\sim 0.5$  m/yr; DeConto et al., 2021). These slow basal velocities are unlikely to have changed significantly since the oldest possible formation age for the silty ice ( $\sim 100$  ka, constrained by the meteoric ice above; Johnsen et al., 1972; Blunier & Brook, 2001), as the ice divide has remained broadly static through the Holocene (Koutnik et al., 2016) and during the last glacial maximum (e.g., Golledge et al., 2012). A constant basal flow velocity of 0.5 m/yr would therefore imply a maximum transport distance of  $\sim 50$  km. Identifying the precise area where the debris was entrained is complicated by local ice flow directions changing at  $\sim 1.5$  ka (Siegert et al., 2004), but the sediment source is likely to have been broadly to the east, somewhere slightly north of Mt. Resnik (Mouginot et al., 2019; Figure S3 in Supporting Information S1).

Our evidence for a subaerial setting close to the Byrd ice core site, which is now well below sea level (Figure 1a; Section S1), provides the first geological evidence supporting paleotopographic reconstructions that imply central West Antarctic topography has been higher in the past (Paxman et al., 2019). Although we cannot constrain when the area was last subaerial, we speculate that this may have been during the Cretaceous, Palaeocene or Eocene, as parts of central West Antarctica had reached sea level by the Eocene (Coenen et al., 2020).

### 3.2. Debris Entrainment

Although all three debris samples have common features, there are subtle mineralogical, geochemical and grain size changes with height in the ice column. For instance, the Upper sample has features such as: a coarser sieved grain size (Table S1 in Supporting Information S1); more monocrystalline grains (e.g., Figure 2); the greatest proportion of sand-sized quartz, pyroxene and zircon grains (Table S2 in Supporting Information S1); a slightly greater smectite content (Figure 3c); and higher  $\epsilon_{\text{Nd}}$  values/lower  $^{87}\text{Sr}/^{86}\text{Sr}$  ratios (Figures 3a and 3b). These changes within the silty ice are likely linked to changes in the composition/lithology of the sedimentary substrate being eroded and entrained. The heterogeneity between samples argues against accretion of the basal ice in a single event and instead suggests entrainment occurred episodically or gradually as the ice moved across the bed, incorporating detritus from different areas. Additionally, retention of debris which was presumably sourced from some distance away excludes the possibility of recent complete melting of the basal debris-rich ice layer.

### 3.3. Evidence for Limited Late Cenozoic Volcanism

Subglacial volcanism has the potential to significantly impact the geothermal heat flux at the bed of the WAIS and thus influence its stability (van Wyk de Vries et al., 2017). Evidence for late Cenozoic volcanism beneath the central WAIS has, however, been limited to a single sample of englacial tephra from the last glacial period (Iverson et al., 2017), supported by geophysical data (e.g., Behrendt, 1999, 2013; van Wyk de Vries et al., 2017). Our new Miocene to recent  $^{40}\text{Ar}/^{39}\text{Ar}$  hornblende ages in the Byrd ice core debris expand this physical record of central West Antarctic volcanism.

However, the low proportion of these ages suggests that Cenozoic volcanic material comprises only a minor fraction of the Byrd ice core debris. This is despite the site's proximity to Mt. Resnik, located only  $\sim 60$  km away (Figure 1; Figure S3 in Supporting Information S1), which is almost certainly a subglacially erupted volcano based on its magnetic anomaly and conical peak (Behrendt, 2013; van Wyk de Vries et al., 2017). Thus, whilst Cenozoic volcanic rocks and recently active volcanoes exist beneath the central WAIS, these likely comprise only a small proportion of the ice sheet substrate, even close to volcanic edifices (Andrews & LeMasurier, 2021; Licht et al., 2005; Perotti et al., 2017; Vogel et al., 2006).

### 3.4. Provenance Signature of the West Antarctic Interior

Greatly reduced WAIS extent would lead to enhanced basal sliding further inland, thus increased basal erosion close to the Byrd ice core location (e.g., Clark et al., 2020; DeConto et al., 2021; DeConto & Pollard, 2016). As the Byrd ice core debris is formed predominantly of reworked sediments, its provenance signature is likely representative of the regional geology that would be eroded during a retreat scenario. Even under complete

deglaciation of the WAIS's marine-based sectors, when the Byrd ice core site would be submarine and not eroded directly (e.g., Figure 1a), erosion of material from nearby topographic highs would carry a similar provenance signature. Modeled ice-sheet trajectories suggest debris eroded from the center of West Antarctica would be transported toward either the Ross Sea and/or the Amundsen Sea, depending on the extent and style of the WAIS collapse (Clark et al., 2020; Goelzer et al., 2016). Recent (Gohl et al., 2021; McKay et al., 2019) and upcoming (Patterson et al., 2022) drill campaigns to the Ross and Amundsen sea sectors aim to search for evidence for major WAIS retreat. The provenance signature of the debris from the Byrd ice core will help test hypotheses of WAIS retreat from these new records.

A powerful provenance constraint from the Byrd ice core debris is the kaolinite content (Balshaw, 1980). In Antarctic seafloor surface sediments, kaolinite is only found in large quantities ( $> \sim 20\%$  of clay minerals) in the Amundsen Sea, where it has been traced to sedimentary rocks in the West Antarctic interior (i.e., Thwaites Glacier catchment, Byrd Subglacial Basin and Bentley Subglacial Trench) which pre-date the onset of Antarctic glaciation (Ehrmann et al., 2011; Hillenbrand et al., 2003; Simões Pereira et al., 2020). The high kaolinite concentration in the Byrd ice core detritus suggests these kaolinite-bearing, pre-glacial sedimentary strata extend close to, or beneath, the Byrd ice core location and are not restricted to the inner shelf region of the Amundsen Sea (Klages et al., 2020). A higher kaolinite content might therefore be expected in sediments deposited in the Ross Sea when the WAIS margin had retreated hundreds of kilometers.

The zircon U-Pb and hornblende  $^{40}\text{Ar}/^{39}\text{Ar}$  data also show features that would be detectable in sediments deposited if there was major WAIS retreat. Late Ross Orogeny ( $\sim 520$ – $475$  Ma) granites and volcanic rocks - potentially reworked through synorogenic metasediments - are likely to be significant contributors to the Byrd debris (Figure 3d; Vogel et al., 2006). However, there is a notable absence of older Ross/Pan African Orogeny zircons of  $\sim 650$ – $520$  Ma age (Figure 3a), which are ubiquitous in sub-ice stream tills and marine sediments in the Ross Sea sector (Licht et al., 2014; Marschalek et al., 2021; Olivetti et al., 2023; Perotti et al., 2017). Rocks of this age must therefore be absent near the Byrd ice core.

The Byrd ice core debris data also show an unusually large fraction of Permian-Early Jurassic ( $\sim 290$ – $180$  Ma) mineral grains compared to sub-ice stream tills and sediments from the Ross (Licht et al., 2014; Marschalek et al., 2021; Olivetti et al., 2023; Perotti et al., 2017) and Amundsen (Simões Pereira et al., 2018, 2020) seas. In all these regions, Permian-Early Jurassic ages are typically a minor contribution; far less than the  $\sim 40\%$  of the zircon U-Pb and  $\sim 33\%$  of the hornblende  $^{40}\text{Ar}/^{39}\text{Ar}$  ages in the Byrd ice core debris. The Permian-Early Jurassic age range is also represented by the  $\sim 218$  Ma rhyolite porphyry clast, which has similar Nd and Sr isotope compositions to the  $< 75$   $\mu\text{m}$  debris fraction (Figure 3; Figure S4 in Supporting Information S1).

The abundance of Permian-Early Jurassic ages measured suggests that the Byrd ice core is proximal to bedrock of this age, or sedimentary strata rich in these rocks. This supports the hypothesis that the presence of Permian-Early Jurassic ages in offshore detrital minerals, despite their absence in coastal rock exposures, means these rocks are most common beneath the central WAIS (Perotti et al., 2017). Retreat of the WAIS would thus likely lead to an increase in mineral grains with an age of  $\sim 290$ – $180$  Ma and a decrease in  $\sim 650$ – $520$  Ma grains shed into the Ross and Amundsen seas.

Detrital neodymium and strontium isotope compositions offer insight into the integrated composition of source rocks eroded from West Antarctica (e.g., Farmer et al., 2006; Simões Pereira et al., 2018). Detrital  $\epsilon_{\text{Nd}}$  values of  $\sim -5$  to  $-7$  measured in sediments from the Ross Sea (Farmer et al., 2006; Marschalek et al., 2021) likely reflect a mixture of Paleozoic metasedimentary rocks similar to those exposed in westernmost Marie Byrd Land (Figure 1b;  $\epsilon_{\text{Nd}} = \sim -11$ ), and a more radiogenic  $\epsilon_{\text{Nd}}$  endmember such as Cenozoic volcanics ( $\epsilon_{\text{Nd}} = \sim +5$ ; see compilation in Simões Pereira et al., 2018). However, the radiogenic endmember could alternatively be Permian-Early Jurassic rocks. Such rocks are abundant within the Byrd ice core debris, as reflected by the mineral ages and measured  $\epsilon_{\text{Nd}}$  values of  $\sim -3$  to  $-4$  of the matrix and clast (Figure 3a). This means that integrated Ross Sea sediment  $\epsilon_{\text{Nd}}$  values can be readily explained by Paleozoic metasedimentary rocks mixing with Permian-Early Jurassic rocks, without a large contribution from Cenozoic volcanics.

In contrast to Cenozoic volcanoes, Permian-Early Jurassic rocks are not currently exposed around the Marie Byrd Land coast (Figure 1b). The source of detritus with more radiogenic  $\epsilon_{\text{Nd}}$  values can therefore be constrained to the West Antarctic interior. Major WAIS retreat may therefore lead to more radiogenic  $\epsilon_{\text{Nd}}$  values and less radiogenic  $^{87}\text{Sr}/^{86}\text{Sr}$  ratios in sediments deposited toward the Ross Sea.



#### 4. Conclusions

Although the Byrd ice core debris has likely only been transported tens of kilometers by the basal ice that entrained it, its provenance signature reflects the broader regional geology as it comprises primarily of detritus derived from pre-Oligocene sedimentary strata. Microtextural, geochemical and mineralogical evidence suggests that these sediments were likely weathered subaerially in a warm climate. This provides the first in situ evidence for a previously subaerial central West Antarctic topography.

Rocks dating to the Permian-Triassic and late Ross Orogeny are major contributors to the Byrd ice core debris. Young volcanic material is also present, supporting evidence for recent volcanism beneath the WAIS. Additionally, subtle changes to the composition of the englacial detritus with height above the ice base suggest the debris was entrained at different points along the flow path.

Crucially, our new data reveal the sediment provenance signature expected for times of major WAIS margin retreat. We provide several testable hypotheses regarding the provenance characteristics of sediments that would be observable in drill records in the Ross or Amundsen Sea drainage sectors during such a scenario. These features are:

- A high proportion of kaolinite in the clay mineral assemblage (~40%).
- Common mineral grains of Permian to Early Jurassic (~290–180 Ma) age.
- Rare/absent mineral grains with an early Ross Orogeny/Pan African Orogeny (~650–520 Ma) age.
- A high  $\epsilon_{\text{Nd}}$  value (~−4) and low  $^{87}\text{Sr}/^{86}\text{Sr}$  ratio (~0.712).

These data may ultimately help determine the timing of the most recent major WAIS retreat as legacy archives are re-examined and new sedimentary records are obtained.

#### Data Availability Statement

This study produced various data sets which have been deposited in Zenodo. These comprise: Nd and Sr isotope compositions (Marschalek and van de Flierdt, 2023; <https://doi.org/10.5281/zenodo.10021918>), clay mineral assemblages (Ehrmann & Marschalek, 2023; <https://doi.org/10.5281/zenodo.10033271>), zircon U-Pb ages (Thomson et al., 2023; <https://doi.org/10.5281/zenodo.10022313>), apatite fission track data (Thomson et al., 2023; <https://doi.org/10.5281/zenodo.10022114>), hornblende  $^{40}\text{Ar}/^{39}\text{Ar}$  ages (Hemming & Marschalek, 2023; <https://doi.org/10.5281/zenodo.10022028>). These data are all freely accessible and licensed under Creative Commons Attribution 4.0.

#### References

- Andrews, J. T., & LeMasurier, W. (2021). Resolving the argument about volcanic bedrock under the West Antarctic Ice Sheet and implications for ice sheet stability and sea level change. *Earth and Planetary Science Letters*, 568, 117035. <https://doi.org/10.1016/j.epsl.2021.117035>
- Arnadóttir, E. Ó., Graly, J. A., Licht, K. J., Bish, D. L., & Caffee, M. W. (2023). Meteoric  $^{10}\text{Be}$  speciation in subglacial sediments of East Antarctica. *Quaternary Geochronology*, 77, 101458. <https://doi.org/10.1016/j.quageo.2023.101458>
- Balshaw, K. M. (1980). *Antarctic glacial chronology reflected in the Oligocene through Pliocene sedimentary section in the Ross Sea (PhD thesis)*. Rice University.
- Behrendt, J. C. (1999). Crustal and lithospheric structure of the West Antarctic Rift System from geophysical investigations—A review. *Global and Planetary Change*, 23(1–4), 25–44. [https://doi.org/10.1016/S0921-8181\(99\)00049-1](https://doi.org/10.1016/S0921-8181(99)00049-1)
- Behrendt, J. C. (2013). The aeromagnetic method as a tool to identify Cenozoic magmatism in the West Antarctic Rift System beneath the West Antarctic Ice Sheet—A review; Thiel subglacial volcano as possible source of the ash layer in the WAISCORE. *Tectonophysics*, 585, 124–136. <https://doi.org/10.1016/j.tecto.2012.06.035>
- Blard, P. H., Protin, M., Tison, J. L., Fripiat, F., Dahl-Jensen, D., Steffensen, J. P., et al., ASTER Team. (2023). Basal debris of the NEEM ice core, Greenland: A window into sub-ice-sheet geology, basal ice processes and ice-sheet oscillations. *Journal of Glaciology*, 69(276), 1–19. <https://doi.org/10.1017/jog.2022.122>
- Blunier, T., & Brook, E. J. (2001). Timing of millennial-scale climate change in Antarctica and Greenland during the last glacial period. *Science*, 291(5501), 109–112. <https://doi.org/10.1126/science.291.5501.109>
- Christoffersen, P., Tulaczyk, S., Carsey, F. D., & Behar, A. E. (2006). A quantitative framework for interpretation of basal ice facies formed by ice accretion over subglacial sediment. *Journal of Geophysical Research*, 111(F1), F01017. <https://doi.org/10.1029/2005JF000363>
- Clark, P. U., He, F., Gollledge, N. R., Mitrovica, J. X., Dutton, A., Hoffman, J. S., & Dendy, S. (2020). Oceanic forcing of penultimate deglacial and last interglacial sea-level rise. *Nature*, 577(7792), 660–664. <https://doi.org/10.1038/s41586-020-1931-7>
- Coenen, J. J., Scherer, R. P., Baudoin, P., Warny, S., Castañeda, I. S., & Askin, R. (2020). Paleogene marine and terrestrial development of the West Antarctic Rift System. *Geophysical Research Letters*, 47(3), e2019GL085281. <https://doi.org/10.1029/2019GL085281>
- Cook, C. P., Van De Flierdt, T., Williams, T., Hemming, S. R., Iwai, M., Kobayashi, M., et al. (2013). Dynamic behaviour of the East Antarctic ice sheet during Pliocene warmth. *Nature Geoscience*, 6(9), 765–769. <https://doi.org/10.1038/ngeo1889>
- Cowan, E. A., Christoffersen, P., & Powell, R. D. (2012). Sedimentological signature of a deformable bed preserved beneath an ice stream in a late Pleistocene glacial sequence, Ross Sea, Antarctica. *Journal of Sedimentary Research*, 82(4), 270–282. <https://doi.org/10.2110/jsr.2012.25>

#### Acknowledgments

We thank Jørgen Peder Steffensen for assisting with the ice core cutting, Katharina Kreissig and Barry Coles (Imperial College London) for support generating the Nd and Sr isotope data, and Sylvia Haeßner (University of Leipzig) for assistance with clay mineral analyses. Jim Marschalek and Tina van de Flierdt acknowledge funding by SSCP Natural Environment Research Council (NERC) DTP and NERC grants NE/R018219/1 and NE/W000172/1. François Fripiat and Lisa Ardoin received funding from the European Union's Horizon 2020 research and innovation programme DEEPICE under the Marie Skłodowska-Curie grant agreement 955750, the FNRS-FRS for the CDR J.0080.22 AEROBIC project, and the subventions Jaumotte-Demoulin for the GENIAL project. Claus-Dieter Hillenbrand and Claire Allen were funded by NERC. We thank Dr Allison Lepp and Dr Trevor Williams for their insightful reviews.

- Cox, S. C., Smith Lyttle, B., Elkind, S., Siddoway, C. S., Morin, P., Capponi, G., et al. (2023). A continent-wide detailed geological map dataset of Antarctica. *Scientific Data*, *10*(1), 250. <https://doi.org/10.1038/s41597-023-02152-9>
- DeConto, R. M., & Pollard, D. (2016). Contribution of Antarctica to past and future sea-level rise. *Nature*, *531*(7596), 591–597. <https://doi.org/10.1038/nature17145>
- DeConto, R. M., Pollard, D., Alley, R. B., Velicogna, I., Gasson, E., Gomez, N., et al. (2021). The Paris Climate Agreement and future sea-level rise from Antarctica. *Nature*, *593*(7857), 83–89. <https://doi.org/10.1038/s41586-021-03427-0>
- Dutton, A., Carlson, A. E., Long, A. J., Milne, G. A., Clark, P. U., DeConto, R., et al. (2015). Sea-level rise due to polar ice-sheet mass loss during past warm periods. *Science*, *349*(6244), aaa4019. <https://doi.org/10.1126/science.aaa4019>
- Dutton, A., & Lambeck, K. (2012). Ice volume and sea level during the last interglacial. *Science*, *337*(6091), 216–219. <https://doi.org/10.1126/science.1205749>
- Ehrmann, W., Hillenbrand, C. D., Smith, J. A., Graham, A. G., Kuhn, G., & Larter, R. D. (2011). Provenance changes between recent and glacial-time sediments in the Amundsen Sea embayment, West Antarctica: Clay mineral assemblage evidence. *Antarctic Science*, *23*(5), 471–486. <https://doi.org/10.1017/S0954102011000320>
- Ehrmann, W., & Marschalek, J. W. (2023). Clay mineralogy of debris from the basal ice of the Byrd ice core, central West Antarctica [Dataset]. Zenodo. <https://doi.org/10.5281/zenodo.10033271>
- Ehrmann, W. U., Melles, M., Kuhn, G., & Grobe, H. (1992). Significance of clay mineral assemblages in the Antarctic Ocean. *Marine Geology*, *107*(4), 249–273. [https://doi.org/10.1016/0025-3227\(92\)90075-S](https://doi.org/10.1016/0025-3227(92)90075-S)
- Farmer, G. L., Licht, K., Swope, R. J., & Andrews, J. (2006). Isotopic constraints on the provenance of fine-grained sediment in LGM tills from the Ross Embayment, Antarctica. *Earth and Planetary Science Letters*, *249*(1–2), 90–107. <https://doi.org/10.1016/j.epsl.2006.06.044>
- Goelzer, H., Huybrechts, P., Loutre, M. F., & Fichefet, T. (2016). Last interglacial climate and sea-level evolution from a coupled ice sheet–climate model. *Climate of the Past*, *12*(12), 2195–2213. <https://doi.org/10.5194/cp-12-2195-2016>
- Gohl, K., Wellner, J. S., & Klaus, A., & the Expedition 379 scientists. (2021). Amundsen Sea West Antarctic ice sheet history. In *Proceedings of the international ocean discovery program*. <https://doi.org/10.14379/iodp.proc.379.2021>
- Golledge, N. R., Fogwill, C. J., Mackintosh, A. N., & Buckley, K. M. (2012). Dynamics of the last glacial maximum Antarctic ice-sheet and its response to ocean forcing. *Proceedings of the National Academy of Sciences*, *109*(40), 16052–16056. <https://doi.org/10.1073/pnas.1205385109>
- Gow, A. J., Epstein, S., & Sheehy, W. (1979). On the origin of stratified debris in ice cores from the bottom of the Antarctic ice sheet. *Journal of Glaciology*, *23*(89), 185–192. <https://doi.org/10.3189/S0022143000029828>
- Gow, A. J., & Meese, D. A. (1996). Nature of basal debris in the GISP2 and Byrd ice cores and its relevance to bed processes. *Annals of Glaciology*, *22*, 134–140. <https://doi.org/10.3189/1996AoG22-1-134-140>
- Gow, A. J., Ueda, H. T., & Garfield, D. E. (1968). Antarctic ice sheet: Preliminary results of first core hole to bedrock. *Science*, *161*(3845), 1011–1013. <https://doi.org/10.1126/science.161.3845.101>
- Graly, J. A., Licht, K. J., Bader, N. A., & Bish, D. L. (2020). Chemical weathering signatures from Mt. Achernar Moraine, Central Transantarctic Mountains I: Subglacial sediments compared with underlying rock. *Geochimica et Cosmochimica Acta*, *283*, 149–166. <https://doi.org/10.1016/j.gca.2020.06.005>
- Hambrey, M. J., Ehrmann, W., & Larsen, B. (1991). Cenozoic glacial record of the Prydz Bay continental shelf, East Antarctica. In J. Barron & B. Larsen (Eds.), *Proceedings of ODP, scientific results* (Vol. 119, pp. 77–132). Ocean Drilling Program. <https://doi.org/10.2973/odp.proc.sr.119.200.1991>
- Hemming, S. R., & Marschalek, J. W. (2023). Hornblende <sup>40</sup>Ar–<sup>39</sup>Ar data from debris from the basal ice of the Byrd ice core, central West Antarctica [Dataset]. Zenodo. <https://doi.org/10.5281/zenodo.10022028>
- Hillenbrand, C. D., Grobe, H., Diekmann, B., Kuhn, G., & Fütterer, D. K. (2003). Distribution of clay minerals and proxies for productivity in surface sediments of the Bellingshausen and Amundsen seas (West Antarctica)–Relation to modern environmental conditions. *Marine Geology*, *193*(3–4), 253–271. [https://doi.org/10.1016/S0025-3227\(02\)00659-X](https://doi.org/10.1016/S0025-3227(02)00659-X)
- Huang, W. H., & Keller, W. D. (1970). Dissolution of rock-forming silicate minerals in organic acids: Simulated first-stage weathering of fresh mineral surfaces. *American Mineralogist: Journal of Earth and Planetary Materials*, *55*(11–12), 2076–2094.
- Iverson, N. A., Lieb-Lappen, R., Dunbar, N. W., Obbard, R., Kim, E., & Golden, E. (2017). The first physical evidence of subglacial volcanism under the West Antarctic Ice Sheet. *Scientific Reports*, *7*(1), 11457. <https://doi.org/10.1038/s41598-017-11515-3>
- Jacobsen, S. B., & Wasserburg, G. J. (1980). Sm–Nd isotopic evolution of chondrites. *Earth and Planetary Science Letters*, *50*(1), 139–155. [https://doi.org/10.1016/0012-821X\(80\)90125-9](https://doi.org/10.1016/0012-821X(80)90125-9)
- Johnsen, S. J., Dansgaard, W., Clausen, H. B., & Langway, C. C. (1972). Oxygen isotope profiles through the Antarctic and Greenland ice sheets. *Nature*, *235*(5339), 429–434. <https://doi.org/10.1038/235429a0>
- Jordan, T. A., Thompson, S., Kulesa, B., & Ferraccioli, F. (2023). Geological sketch map and implications for ice flow of Thwaites Glacier, West Antarctica, from integrated aerogeophysical observations. *Science Advances*, *9*(22), eadf2639. <https://doi.org/10.1126/sciadv.adf2639>
- Klages, J. P., Salzmann, U., Bickert, T., Hillenbrand, C. D., Gohl, K., Kuhn, G., et al., Science Team of Expedition PS104. (2020). Temperate rainforests near the South Pole during peak Cretaceous warmth. *Nature*, *580*(7801), 81–86. <https://doi.org/10.1038/s41586-020-2148-5>
- Korhonen, F. J., Saito, S., Brown, M., Siddoway, C. S., & Day, J. M. D. (2010). Multiple generations of granite in the Fosdick Mountains, Marie Byrd Land, West Antarctica: Implications for polyphase intracrustal differentiation in a continental margin setting. *Journal of Petrology*, *51*(3), 627–670. <https://doi.org/10.1093/ptrology/egp093>
- Koutnik, M. R., Fudge, T. J., Conway, H., Waddington, E. D., Neumann, T. A., Cuffey, K. M., et al. (2016). Holocene accumulation and ice flow near the West Antarctic Ice Sheet Divide ice core site. *Journal of Geophysical Research: Earth Surface*, *121*(5), 907–924. <https://doi.org/10.1002/2015JF003668>
- Li, X., Zattin, M., & Olivetti, V. (2020). Apatite fission track signatures of the Ross Sea ice flows during the Last Glacial Maximum. *Geochemistry, Geophysics, Geosystems*, *21*(10), e2019GC008749. <https://doi.org/10.1029/2019GC008749>
- Licht, K. J., Hennessy, A. J., & Welke, B. M. (2014). The U–Pb detrital zircon signature of West Antarctic ice stream tills in the Ross embayment, with implications for Last Glacial Maximum ice flow reconstructions. *Antarctic Science*, *26*(6), 687–697. <https://doi.org/10.1017/S0954102014000315>
- Licht, K. J., Lederer, J. R., & Swope, R. J. (2005). Provenance of LGM glacial till (sand fraction) across the Ross embayment, Antarctica. *Quaternary Science Reviews*, *24*(12–13), 1499–1520. <https://doi.org/10.1016/j.quascirev.2004.10.017>
- Mahaney, W. C. (1995). Pleistocene and Holocene glacier thicknesses, transport histories and dynamics inferred from SEM microtextures on quartz particles. *Boreas*, *24*(4), 293–304. <https://doi.org/10.1111/j.1502-3885.1995.tb00781.x>
- Mahaney, W. C. (2002). *Atlas of sand grain surface textures and applications*. Oxford University Press.
- Marschalek, J. W., & van de Fliert, T. (2023). Neodymium and strontium isotope compositions of debris from the basal ice of the Byrd ice core, central West Antarctica [Dataset]. Zenodo. <https://doi.org/10.5281/zenodo.10021918>

- Marschalek, J. W., Zurli, L., Talarico, F., van de Flierdt, T., Vermeesch, P., Carter, A., et al. (2021). A large West Antarctic Ice Sheet explains early Neogene sea-level amplitude. *Nature*, 600(7889), 450–455. <https://doi.org/10.1038/s41586-021-04148-0>
- McKay, R., De Santis, L., & Kulhanek, D. K., & the Expedition 374 Science Party. (2019). Ross Sea West Antarctic Ice Sheet history. In *Proceedings of the international ocean discovery program*. <https://doi.org/10.14379/iocdp.proc.374.2019>
- Morlighem, M., Rignot, E., Binder, T., Blankenship, D., Drews, R., Eagles, G., et al. (2020). Deep glacial troughs and stabilizing ridges unveiled beneath the margins of the Antarctic ice sheet. *Nature Geoscience*, 13(2), 132–137. <https://doi.org/10.1038/s41561-019-0510-8>
- Mouginot, J., Rignot, E., & Scheuchl, B. (2019). Continent-wide, interferometric SAR phase-mapping of Antarctic ice velocity. *Geophysical Research Letters*, 46(16), 9710–9718. <https://doi.org/10.1029/2019GL083826>
- Mouginot, J., Scheuchl, B., & Rignot, E. (2017). *MEASUREs Antarctic boundaries for IPY 2007-2009 from satellite radar, version 2*. Boulder, Colorado USA. NASA National Snow and Ice Data Center Distributed Active Archive Center. <https://doi.org/10.5067/AXE4121732AD>
- Olivetti, V., Balestrieri, M. L., Chew, D., Zurli, L., Zattin, M., Pace, D., et al. (2023). Ice volume variations and provenance trends in the Oligocene-early Miocene glaciomarine sediments of the Central Ross Sea, Antarctica (DSDP site 270). *Global and Planetary Change*, 221, 104042. <https://doi.org/10.1016/j.gloplacha.2023.104042>
- Patterson, M. O., Levy, R. H., Kulhanek, D. K., van de Flierdt, T., Horgan, H., Dunbar, G. B., et al. (2022). Sensitivity of the West Antarctic Ice Sheet to +2°C (SWAIS 2C). *Scientific Drilling*, 30, 101–112. <https://doi.org/10.5194/sd-30-101-2022>
- Paxman, G. J., Jamieson, S. S., Hochmuth, K., Gohl, K., Bentley, M. J., Leitchenkov, G., & Ferraccioli, F. (2019). Reconstructions of Antarctic topography since the Eocene–Oligocene boundary. *Palaeogeography, Palaeoclimatology, Palaeoecology*, 535, 109346. <https://doi.org/10.1016/j.palaeo.2019.109346>
- Perotti, M., Andreucci, B., Talarico, F., Zattin, M., & Langone, A. (2017). Multianalytical provenance analysis of Eastern Ross Sea LGM till sediments (Antarctica): Petrography, geochronology, and thermochronology detrital data. *Geochemistry, Geophysics, Geosystems*, 18(6), 2275–2304. <https://doi.org/10.1002/2016GC006728>
- Petschick, R., Kuhn, G., & Gingele, F. X. (1996). Clay mineral distribution in surface sediments of the South Atlantic: Sources, transport, and relation to oceanography. *Marine Geology*, 130(3–4), 203–229. [https://doi.org/10.1016/0025-3227\(95\)00148-4](https://doi.org/10.1016/0025-3227(95)00148-4)
- Rignot, E., Jacobs, S., Mouginot, J., & Scheuchl, B. (2013). Ice-shelf melting around Antarctica. *Science*, 341(6143), 266–270. <https://doi.org/10.1126/science.1235798>
- Robert, C., & Kennett, J. P. (1994). Antarctic subtropical humid episode at the Paleocene-Eocene boundary: Clay-mineral evidence. *Geology*, 22(3), 211–214. [https://doi.org/10.1130/0091-7613\(1994\)022<0211:ASHEAT>2.3.CO;2](https://doi.org/10.1130/0091-7613(1994)022<0211:ASHEAT>2.3.CO;2)
- Scherer, R. P., Aldahan, A., Tulaczyk, S., Possnert, G., Engelhardt, H., & Kamb, B. (1998). Pleistocene collapse of the West Antarctic ice sheet. *Science*, 281(5373), 82–85. <https://doi.org/10.1126/science.281.5373.82>
- Siebert, M. J., Welch, B., Morse, D., Viel, A., Blankenship, D. D., Joughin, I., et al. (2004). Ice flow direction change in interior West Antarctica. *Science*, 305(5692), 1948–1951. <https://doi.org/10.1126/science.1101072>
- Simões Pereira, P., van de Flierdt, T., Hemming, S. R., Frederichs, T., Hammond, S. J., Brachfeld, S., et al. (2020). The geochemical and mineralogical fingerprint of West Antarctica's weak underbelly: Pine Island and Thwaites glaciers. *Chemical Geology*, 550, 119649. <https://doi.org/10.1016/j.chemgeo.2020.119649>
- Simões Pereira, P., van de Flierdt, T., Hemming, S. R., Hammond, S. J., Kuhn, G., Brachfeld, S., et al. (2018). Geochemical fingerprints of glacially eroded bedrock from West Antarctica: Detrital thermochronology, radiogenic isotope systematics and trace element geochemistry in Late Holocene glacial-marine sediments. *Earth-Science Reviews*, 182, 204–232. <https://doi.org/10.1016/j.earscirev.2018.04.011>
- Storey, B. C., & MacDonald, D. I. M. (1987). Sedimentary rocks of the Ellsworth-Thiel Mountains ridge and their regional equivalents. *Bulletin of the British Antarctic Survey*, 76, 21–49.
- Thomson, S. N., Marschalek, J. W., & Licht, K. (2023). Apatite fission track data from debris from the basal ice of the Byrd ice core, central West Antarctica [Dataset]. Zenodo. <https://doi.org/10.5281/zenodo.10022114>
- Thomson, S. N., Marschalek, J. W., & Licht, K. (2023). Zircon U-Pb ages of debris from the basal ice of the Byrd ice core, central West Antarctica [Dataset]. Zenodo. <https://doi.org/10.5281/zenodo.10022313>
- van Wyk de Vries, M., Bingham, R. G., & Hein, A. S. (2017). A new volcanic province: An inventory of subglacial volcanoes in West Antarctica. *Geological Society, London, Special Publications*, 461(1), 231–248. <https://doi.org/10.1144/SP461.7>
- Vermeesch, P. (2012). On the visualisation of detrital age distributions. *Chemical Geology*, 312, 190–194. <https://doi.org/10.1016/j.chemgeo.2012.04.021>
- Vogel, S. W. (2004). *The basal regime of the West-Antarctic ice sheet interaction of subglacial geology with ice dynamics [PhD Thesis]*. University of California.
- Vogel, S. W., Tulaczyk, S., Carter, S., Renne, P., Turrin, B., & Grunow, A. (2006). Geologic constraints on the existence and distribution of West Antarctic subglacial volcanism. *Geophysical Research Letters*, 33(23), L23501. <https://doi.org/10.1029/2006GL027344>
- Weaver, S. D., Adams, C. J., Pankhurst, R. J., & Gibson, I. L. (1992). Granites of Edward VII Peninsula, Marie Byrd Land: Anorogenic magmatism related to Antarctic-New Zealand rifting. *Transactions of the Royal Society of Edinburgh Earth Sciences*, 83(1–2), 281–290. <https://doi.org/10.1017/S0263593300007963>
- Windom, H. L. (1976). Lithogenous material in marine sediments. In J. P. Riley & R. Chester (Eds.), *Chemical oceanography* 5 (pp. 103–135). Academic Press.

## References From the Supporting Information

- Cailleux, A., & Tricart, J. (1959). *Initiation à l'étude des sables et des galets*. Centre de la Documentation Universitaire.
- Chaput, J., Aster, R. C., Huerta, A., Sun, X., Lloyd, A., Wiens, D., et al. (2014). The crustal thickness of West Antarctica. *Journal of Geophysical Research: Solid Earth*, 119(1), 378–395. <https://doi.org/10.1002/2013JB010642>
- Donelick, R. A., O'Sullivan, P. B., & Ketcham, R. A. (2005). Apatite fission-track analysis. *Reviews in Mineralogy and Geochemistry*, 58(1), 49–94. <https://doi.org/10.2138/rmg.2005.58.3>
- Galbraith, R. F. (2005). *Statistics for fission track analysis*. CRC Press.
- Galbraith, R. F., & Laslett, G. M. (1993). Statistical models for mixed fission track ages. *Nuclear Tracks and Radiation Measurements*, 21(4), 459–470. [https://doi.org/10.1016/1359-0189\(93\)90185-c](https://doi.org/10.1016/1359-0189(93)90185-c)
- Gehrels, G. E., Valencia, V. A., & Ruiz, J. (2008). Enhanced precision, accuracy, efficiency, and spatial resolution of U-Pb ages by laser ablation–multicollector–inductively coupled plasma–mass spectrometry. *Geochemistry, Geophysics, Geosystems*, 9(3), Q03017. <https://doi.org/10.1029/2007gc001805>

- Gleadow, A. J. W. (1981). Fission-track dating methods: What are the real alternatives? *Nuclear Tracks*, 5(1–2), 3–14. [https://doi.org/10.1016/0191-278x\(81\)90021-4](https://doi.org/10.1016/0191-278x(81)90021-4)
- Gutjahr, M., Frank, M., Stirling, C. H., Klemm, V., van de Fliedert, T., & Halliday, A. N. (2007). Reliable extraction of a deepwater trace metal isotope signal from Fe–Mn oxyhydroxide coatings of marine sediments. *Chemical Geology*, 242(3–4), 351–370. <https://doi.org/10.1016/j.chemgeo.2007.03.021>
- Hurford, A. J. (1990). Standardization of fission track dating calibration: Recommendation by the fission track working group of the IUGS subcommission on geochronology. *Chemical Geology: Isotope Geoscience section*, 80(2), 171–178. [https://doi.org/10.1016/0168-9622\(90\)90025-8](https://doi.org/10.1016/0168-9622(90)90025-8)
- Hurford, A. J., & Green, P. F. (1983). The zeta age calibration of fission-track dating. *Chemical Geology*, 41, 285–317. [https://doi.org/10.1016/s0009-2541\(83\)80026-6](https://doi.org/10.1016/s0009-2541(83)80026-6)
- Kuiper, K. F., Deino, A., Hilgen, F. J., Krijgsman, W., Renne, P. R., & Wijbrans, A. J. (2008). Synchronizing rock clocks of Earth history. *Science*, 320(5875), 500–504. <https://doi.org/10.1126/science.1154339>
- Li, L., Aitken, A. R., Lindsay, M. D., & Kulesa, B. (2022). Sedimentary basins reduce stability of Antarctic ice streams through groundwater feedbacks. *Nature Geoscience*, 15(8), 645–650. <https://doi.org/10.1038/s41561-022-00992-5>
- Paxman, G. J., Austermann, J., & Hollyday, A. (2022). Total isostatic response to the complete unloading of the Greenland and Antarctic Ice Sheets. *Scientific Reports*, 12(1), 1–10. <https://doi.org/10.1038/s41598-022-15440-y>
- Renne, P. R. (1995). Excess <sup>40</sup>Ar in biotite and hornblende from the Noril'sk 1 intrusion, Siberia: Implications for the age of the Siberian Traps. *Earth and Planetary Science Letters*, 131(3–4), 165–176. [https://doi.org/10.1016/0012-821x\(95\)00015-5](https://doi.org/10.1016/0012-821x(95)00015-5)
- Tanaka, T., Togashi, S., Kamioka, H., Amakawa, H., Kagami, H., Hamamoto, T., et al. (2000). JNd-1: A neodymium isotopic reference in consistency with LaJolla neodymium. *Chemical Geology*, 168(3–4), 279–281. [https://doi.org/10.1016/s0009-2541\(00\)00198-4](https://doi.org/10.1016/s0009-2541(00)00198-4)
- Vermeesch, P. (2018). IsoplotR: A free and open toolbox for geochronology. *Geoscience Frontiers*, 9(5), 1479–1493. <https://doi.org/10.1016/j.gsf.2018.04.001>
- Vermeesch, P. (2021). On the treatment of discordant detrital zircon U–Pb data. *Geochronology*, 3(1), 247–257. <https://doi.org/10.5194/gchron-3-247-2021>
- Weis, D., Kieffer, B., Maerschalk, C., Barling, J., De Jong, J., Williams, G. A., et al. (2006). High-precision isotopic characterization of USGS reference materials by TIMS and MC-ICP-MS. *Geochemistry, Geophysics, Geosystems*, 7(8), Q08006. <https://doi.org/10.1029/2006gc001283>